The Harpy

40th Annual VFS Student Design Competition

High-Speed Vertical Take-Off and Landing (HSVTOL) Aircraft

Sponsored by Sikorsky

Georgia Tech

Daniel Guggenheim School of Aerospace Engineering
Georgia Institute of Technology
Atlanta, GA, 30332

UNITED STATES MILITARY ACADEMY
WEST POINT

Department of Civil & Mechanical Engineering
United States Military Academy at West Point
West Point, NY, 10996

Daniel Guggenheim School
of Aerospace Engineering
Georgia Institute of Technology
Atlanta, GA, 30332

Department of Civil
& Mechanical Engineering
United States Military Academy
at West Point
West Point, NY, 10996

40th Annual Vertical Flight Society Student Design Competition

Undergraduate Category

Abinay Brown – *Undergraduate Student* *
Fixed Wing Aerodynamic Analysis
abrown472@gatech.edu
Georgia Institute of Technology

Walther Chong – *Undergraduate Student* *
Team Leader
wchong34@gatech.edu
Georgia Institute of Technology

William Henry – *Undergraduate Student* ^
Rotary Wing & Propulsion
william.henry@westpoint.edu
United States Military Academy at West Point

Maxwell Hoem – *Undergraduate Student* **
Systems Design & Propulsion
mhoem3@gatech.edu
Georgia Institute of Technology

Gray Simmons – *Undergraduate Student* **
CAD & Aerodynamic Design
gsimmons9@gatech.edu
Georgia Institute of Technology

Anisha Singh – *Undergraduate Student* **
Materials & Manufacturing
asingh704@gatech.edu
Georgia Institute of Technology

Course Credit

* AE4863, GT Special Topic
** AE4343, GT Rotorcraft Design
^ ME389, WP Adv. Studies

Andrew Sohn – *Undergraduate Student* **
Aerodynamic Design & Structures
andrew.sohn@gatech.edu
Georgia Institute of Technology

Dr. Marilyn J. Smith – *Faculty Advisor*
marilyn.smith@ae.gatech.edu
Georgia Institute of Technology

Dr. Chance C. McColl – *Faculty Advisor*
chance@gatech.edu
Georgia Institute of Technology

Dr. Robert Walters – *Faculty Advisor*
robert.walters@westpoint.edu
United States Military Academy at West Point

Daniel Guggenheim School
of Aerospace Engineering
Georgia Institute of Technology
Atlanta, GA, 30332

Department of Civil
& Mechanical Engineering
United States Military Academy
at West Point
West Point, NY, 10996

To the Vertical Flight Society:

The members of the combined Georgia Institute of Technology-West Point Undergraduate Student Design Team, hereby grant VFS full permission to distribute the enclosed Executive Summary and Final Proposal for the 40th Annual Design Competition as they see fit.

Thank you,

The Georgia Tech-West Point Undergraduate Design Team

Acknowledgements

The Georgia Tech Design Team would like to thank those who were able to answer our general technical questions during the team's design process.

Georgia Tech Faculty

Dr. Juergen Rauleder
Assistant Professor and Associate Director of Vertical Lift Research Center of Excellence, Daniel Guggenheim School of Aerospace Engineering, Georgia Institute of Technology

Dr. Marilyn J. Smith
Professor and Director of Vertical Lift Research Center of Excellence, Daniel Guggenheim School of Aerospace Engineering, Georgia Institute of Technology

Dr. Chance C. McColl
Lecturer, Daniel Guggenheim School of Aerospace Engineering, Georgia Institute of Technology

West Point Faculty

Dr. Robert Walters
Assistant Professor, Department of Civil & Mechanical Engineering, United States Military Academy at West Point

Georgia Tech Teaching Assistants

Ms. Carlota Bonnet
PhD Candidate & Teaching Assistant, Daniel Guggenheim School of Aerospace Engineering, Georgia Institute of Technology

Mr. Derek Safieh
PhD Candidate & Teaching Assistant, Daniel Guggenheim School of Aerospace Engineering, Georgia Institute of Technology

Table of Contents

List of Figures

List of Tables

Nomenclature

AHP Analytical Hierarchy Process

CSAR Combat Search and Rescue

DL Disk Loading

GL Ground Level

h_{BC} Best Cruise Altitude

HIGE Hover In Ground E ect

HOGE Hover Out of Ground E ect

MMGW Mid-Mission Gross Weight

MRP Maximum Rated Power

NOE Nap of the Earth

OEI One Engine Inoperable

RFP Request for Proposal

SDGW Structural Design Gross Weight

SMR Single Main Rotor

V_{BROC} Best Rate of Climb Speed

V_{BR} Best Range Speed

V_{MCP} Maximum Continuous Power Speed

Harpy RFP Requirements and Compliances

RFP Requirement	Solution	Section
The vehicle shall have an internal cargo bay with dimensions of 6.5 ft (1.98 m) high, 8 ft (2.43 m) wide, 30 ft (9.14 m) long	Cargo Bay has minimum dimensions of 6.5 ft (1.98 m) by 10.5 ft (3.2 m) by 33 ft (10.1 m)	10
SDGW shall be de ned as the TOGW of the Primary Mission illustrated in Fig. 3 while carrying 5,000 lb (2,258 kg) of Payload and a Mission Equipment Package (MEP) of 1,000 lb (454 kg).	The required lift for trim ight was adjusted	11
Airframe limit n shall be 3.5g at SDGW.	Additional Structure added to maintain integrity	8
Landing Gear shall be designed for a sink speed of 10 ft/s (3.0 m/s) at SDGW with 2/3 rotor lift.	Size and de ection designed to meet requirement	8
The aircraft shall be able to y 450 KTAS (833 km/h) at 20,000 ft (6,096 m) MSL ISA conditions using no more than 100% MCP or 100% maximum continuous torque from the primary propulsion system at SDGW	Powerplant system selected to satisfy minimum thrust	5
The aircraft shall have a mission ROA of 500 nm (926 km) while carrying 5,000 lb (2,268 kg) payload and 1,000 lb (454 kg) MEP, comprised of 450 nm (833 km) of cruise speed greater than 450 KTAS (833 km/h) at no less than 20,000 ft (6,096 m) MSL ISA and 50 nm (92.6 km) of cruise speed at the propulsion system's MCP at an ambient condition of 2,000 ft MSL 85°F.	Powerplant and fuel storage included to meet requirement	5
The aircraft shall be capable of executing a HOGE at the mid-mission segment of the Primary Mission using no more than 90% of the engine MRP or 100% of the gearbox and/or motor torque at an ambient condition of 2,000ft (609.6m) MSL and 85°F (24°C).	Rotor and Convertible Engine designed/chosen to meet requirement	5, 9
The vehicle design shall include features to mitigate the severity of the outwash/downwash environment on ground personnel. The disk loading of the vehicle shall not exceed 40 psf (1.9 kPa).	Research conducted to determine requirement and Rotor designed to these requirement	5, 7
The vehicle design shall include features to minimize susceptibility of the propulsion system to FOD ingestion during VTOL ops.	Rotor designed to minimize disk loading, downwash, and outwash	5, 7

1 Introduction

The concept of combining the vertical ight capability a orded by rotary wing aircraft and the long range and high speed capabilities of xed wing aircraft has been of interest since the 1920s and 1930s, predating the success of production helicopters introduced by Igor Sikorsky in the 1940s by at least a decade [5].

Early High-Speed Vertical Take-O and Landing (HSVTOL) vehicle designs were not successful as technology maturation and experience with Vertical Take-O and Landing (VTOL) vehicles were required. Currently, higher-speed VTOL vehicles such as the McDonnell Douglas (Boeing) AV-8B Harrier or the Lockheed F-35 Lightning II in the attack role or the Bell-Boeing V-22 Osprey for transport roles play a vital role in the U.S. military. They do have limitations. The thrust-vectored jet aircraft have very high downwash and equivalent disk loading (DL) due to the use of directed jet thrust, and while the V-22 has seen large success in its role as a higher speed VTOL transport aircraft, its maximum speed is still limited by its large prop-rotors, preventing it from being able to reach transonic speeds and altitudes comparable to xed-wing transport aircraft.

The challenge therein comes in balancing the hovering rotor requirements and the low-parasitic drag required to e ciently cruise at high speeds. In hover, larger rotors will minimize downwash and outwash during operations in harsh and unprepared surfaces to reduce risk to ground personnel and foreign object debris (FOD) ingestion. High speed cruise conventionally reduces rotor size due to the large drag and overall ine ciency of rotors in horizontal propulsion.

Harpy, named after the mythological hybrid human-bird personi cation of storm winds as well as the Harpy Eagle, one of the strongest birds in lifting capacity, is a hybrid rotary- xed wing vehicle concept designed to not only lift large payloads, but also to carry it faster and farther than previously achieved for a vertical lift transport concept. The hybrid concept in this case refers to the convertiplane nature of the concept which operates in two distinct ight con gurations for vertical ight and high-speed forward ight respectively. Harpy is a side-by-side rotary-wing vehicle during vertical ight modes and transforms into a xed-wing vehicle via anovel stopped and stowed rotor concept wherein the rotors are integrated into the main xed wing during high speed ight. A convertible turboshaft engine acts to drive the rotors in hover, transforming to a turbofan in forward ight. This unique design solution leverages the optimal hovering and low DL characteristics of rotor-based vertical ight solutions with performance of a conventional xed-wing solution in high-speed forward ight. Thus, Harpy is capable of not only high-speed ight, but also gives room for expansion into more diverse mission pro les that may require the low observability and aerial refueling tasks that require operations in its xed-wing mode. The latter permits interfacing with a more diverse range of tankers due to the larger ight envelope, as well as reducing the risk of inadvertent damage to refueling equipment due to rotors. Recall, the rotors are stopped and stowed in xed-wing ight.

2 Concept of Operations

2.1 Operational Requirements

Requirement	Satis ed?	Chapter
Payload	Met	5
Internal Cargo Size	Met	10
Hover (HIGE/HOGE) Capable	Exceeded	5
Range	Met	5
Altitude	Met	5
Level Flight Speed	Met	5
Downwash	Met	7
FOD Mitigation	Met	9

Table 2.1 System requirement table, emphasized requirements are soft requirements

2.2 Mission Pro le

The RFP mission pro le has been equivalently reproduced in Figure 2.1 with repeated segment shown for clarity. The ground level (GL) was elevated at 2,000 ft (609.6 m) MSL at 85 F (29.44 C), denoting a hot and high ground level condition. The mission begins in segment 1 at the Structural Design Gross Weight (SDGW) , de ned as initial take-o weight, with a 10 minute ight idle for warm-up, followed by a 2 minute Hover In Ground E ect (HIGE) in segment 2, the vehicle then climbs to a minimum threat avoidance altitude of 20,000 ft (6,096 m) MSL at ISA conditions at best rate of climb speed (V_{BROC}) in segment 3, allowing for the best climb performance. Range credit is applied during the climb and thus may constitute a part of the 500 nm (926 km) radius of action (ROA) required. Once at altitude, the high-speed cruise phase, segment 4, begins with a minimum of 450 KTAS (833.4 km/h) or best cruise, whichever is greater, at best cruise altitude (h_{BC}) or 20,000 ft (6,096 m) ISA, whichever is greater, for a radius of action of 450 nm (833.4 km). Mission segment 5 consists of a descent with no range credit applied, illustrated as a spiral descent to ground level conditions in Figure 2.1, segment 6 then begins the high speed penetration phase at ground level conditions at maximum continuous power speed (V_{MCP}) for the remaining 50 nm (92.6 km) of the ROA. The vehicle is then brought to a 2 minute Hover Out of Ground E ect (HOGE) at a mid-mission landing zone in segment 7. The vehicle's gross weight at the beginning of segment 7 is the SDGW less fuel burned through segments 1 6 which is denoted as the Mid-Mission Gross Weight (MMGW) . Segments 3 7 are repeated once more at MMGW for the return leg of the mission. Energy reserves are de ned as 20 minutes at best range speed (V_{BR}) under ground level conditions. A summary of the mission segments is represented in tabular form for convenience in Table 2.2.

Figure 2.1 HSVTOL mission pro le

	Mission Segment	Characteristics	Conditions
1	Flight Idle	10 min	SDGW, GL
2	HIGE	2 min	SDGW, GL
3	Steady Climb to max{h_{BC}, 20,000 ft (6,096 m)}	V_{BROC}, Range Credit to ROA	SDGW, ISA
4	High-Speed Cruise at max{h_{BC}, 20,000 ft (6,096 m)}	450 nm (833.4 km) @max{V_{BR}, 450 KTAS (231.5 m/s)}	SDGW, ISA
5	Descend to GL	No Range Credit	SDGW, GL
6	High-Speed Penetration	50 nm (92.6 km) @V_{MCP}	SDGW, GL
7	HOGE	2 min	MMGW, GL
3	Steady Climb to max{h_{BC}, 20,000 ft (6,096 m)}	V_{BROC}, Range Credit to ROA	MMGW, ISA
4	High-Speed Cruise at max{h_{BC}, 20,000 ft (6,096 m)}	450 nm (833.4 km) @max{V_{BR}, 450 KTAS (231.5 m/s)}	MMGW, ISA
5	Descend to GL	No Range Credit	MMGW, GL
6	High-Speed Penetration	50 nm (92.6 km) @V_{MCP}	MMGW, GL
7	HOGE	2 min, 20 min Reserves @V_{BR}	GL

Table 2.2 Mission pro le summary. GL: 2,000 ft (609.6 m) at 85 F (29.44 C), ROA: 500 nm (926 km)

3 Preliminary Con guration Selection

3.1 Mission Requirements

3.1.1 Design Objectives

The mission pro le and operating conditions set out by the requirements of the Request for Proposal (RFP) motivate the design objectives presented in this section. Each design objective is introduced with a description of its role in ful lling the mission requirements.

Con guration Design Objectives:

- Cruise Performance: The vehicle must be capable of sustained cruise speeds at or in excess of 450 KTAS at a minimum altitude of 20,000 ft (6096 m) ISA conditions without exceeding 100% propulsion output and/or transmission torque.

  The high altitude cruise segment shall be carried out at best cruise altitude and best cruise speed of 450 KTAS amd 20,000 ft, whichever is greater. A low altitude high speed penetration at ground level conditions of 2,000 ft (609.6 m) MSL at 85 F (29 C) is also required at the speed of maximum continuous power as per the request for proposal (RFP).

- Hover Performance: The vehicle must be capable of 2 minute segments of hover in ground e ect (HIGE) and hover out of ground e ect (HOGE) at an elevated ground level of 2,000 ft (609.6 m) MSL and 85 F (29 C) ambient temperature. The low outwash and downwash requirement and the unprepared surface operation to reduce FOD ingestion motivates disk loading to below 40 psf (1,915 N/m^2), the design limit was determined as maximum of 25 psf (1,197 N/m^2) determined by the Combat Search and Rescue (CSAR) mission requirement [6].

  At the mid-mission segment the vehicle shall hover OGE at or below 90% maximum rated power (MRP) or 100% transmission and/or motor torque.

- Environmental Susceptibility/Survivability: Since the vehicle must operate from unprepared surfaces, the possibility of dust and dirt ingress as well as brownout conditions were considered in the design and minimizing FOD ingestion was taken into consideration with air breathing engine intake placement.

- Adaptability: The need to ful ll competing roles during the course of the mission necessitates the ability to adapt to the speci c needs and challenges of each mission segment. This design objective encompasses

not only the capability of ful lling each mission segment, but also the delicate balance between them. In the context of a convertiplane, this manifests frequently as the transition speed between the phases of ight. The adaptability of the vehicle corresponds to a metric that weights its hover performance and cruise performance to each other; proportioning the performance in each to a scale of 0 to 1 into a score based on performance metrics such as FM, DL, and max level ight speed. As hover and forward ight segments are not equally weighted in terms of time spent in each phase, where forward ight vastly outweighs that of hover, a weight is applied to the scores to re ect the mission balance in the vehicle.

- Maneuverability: A vehicle operating in highly contested environments must be able to avoid threats by performing defensive and evasive maneuvers such as Nap-Of-the-Earth (NOE) ight which constitutes of dynamic banking and climbing maneuvers, as such the design should encompass maneuverability for at least 3.5 g load factor as well as rates of climbs in excess of 1,000 ft/min (304.8 m/min) to allow rapid climb to threat avoidance altitude when needed. Maneuverability also encompasses factors such as high angular rates, particularly in the pitch and roll axes, which allows the vehicle to change the direction of its lift vector quickly on top of being able to handle a large magnitude as would be seen in steady maneuvers. Maneuverability in all con gurations can be considered in the form of maximum angular rate in each con guration.

- Mission Readiness: Vehicles operating in harsh environments and from unprepared surfaces often do not have access to the wealth of logistics a orded by vehicles that operate predominantly from a base such as an airbase or an aircraft carrier, design considerations were taken to improve reliability of systems by making critical systems accessible for eld servicing as well as protected from damage when not being operated. This is commonly seen in the form of gust locks and stowable components to reduce the potential of damage during transport, panels that are accessible by trained ground crew that do not require specialized tooling, as well as easily observable mechanisms and uid levels. Critical systems should be easily inspectable and accessible for regular maintenance even when operating from an o - eld site.

- Structural Complexity: The vehicle must be capable of sustaining a minimum of 3.5g structural load factor, and the structure of the vehicle should be designed in a manner that reduces its form factor and impingement upon other vital systems. Structural complexity also encompasses factors such as the mass distribution of the vehicle, which a ects the moment of inertia and thus the controllability of the vehicle in terms of control force necessary to maneuver as well as the angular rates of the vehicle during dynamic maneuvers.

- System Complexity: The design of the vehicle should be elegant and simple wherever possible, improving the reliability of the system and reducing points of failure as well as increasing the feasibility of the vehicle concept. Novel concepts, techniques, as well as approaches to existing methods that reduce overall operational complexity and provide functional redundancy are favored over systems with large quantities of co-dependent interfaces.

Propulsion Design Objectives:

- Speci c Power: Speci c power is considered as a power output of propulsion system per unit mass. A propulsion system here includes propulsor, energy source, and all associated routing of energy from source to propulsor, as well as power transmission devices such as driveshafts and gearboxes. As an example, for a conventional air-breathing propulsion system, a propulsor would denote a turboshaft engine, and the energy source would mean JET A-1 fuel. An electrical system would be slightly di erent in a sense that the propulsor now becomes an electric motor and the energy source would mean batteries. The more power the overall system can produce per unit mass, the system would enjoy the bene t of having less mass for its propulsion system while meeting the power requirements.

- Volumetric Energy Density: For the storage of energy source, such as petroleum-based fuel, chemical batteries, and hydrogen tanks, energy-volume relationship describes how much energy can be stored per unit volume. Better volumetric energy density performance will bene t the design by saving space allocated to energy storage.

- Speci c Energy: A performance metric of energy per mass of energy source is considered as another deign objective for propulsion system. This metric applies to the di erent types of energy storage, and better speci c energy performance would mean that the system is storing required amount of energy for the propulsion system with less mass dedicated to it.
- Versatility/Flexibility: Energy source and engine con guration/role/duties/functional redundancy The propulsion system's versatility and exibility with regards to energy sources and engine con guration considers the range of roles, con guration, and functional redundancy of the system. A system that can work o of multiple types of energy sources will be considered as a more versatile option. Also, as the vehicle must operate in wide range of ight conditions, the ability to satisfy propulsion requirement in all ight envelope with same propulsion system is highly desired. Additionally, a system's function could provide functional redundancy, which further improves the system's versatility and exibility.
- Environmental Resilience: The design of the propulsion system must be able to withstand adverse e ects from Foreign Object Debris (FOD) ingestion, mainly originating from operation over unprepared surfaces. Additionally, the design should consider any possible power lapse due to air density change, and e ects resulting from temperature lapse, mainly from altitude change.
- E ciency: The propulsion system design must consider the e ciency of its propulsor. As di erent propulsion system has di erent e ciency metrics associated with it, the most comparable metrics are selected for di erent type of propulsor. For engines associated with thermal cycle, thermal e ciency is considered. For electric motors, motor e ciency is considered.
- Mechanical Complexity: A design of propulsion system must give careful consideration of moving parts, gearboxes, and linkages as such features inevitably increases unit cost, manufacturing complexity, production time, and has higher chance of hindering maintainability and robustness. A simpler system con guration may be more feasible in a sense that there is better control over system reliability and reducing points of failure.

3.1.2 Analytical Hierarchy Process (AHP)

AHP matrices were used to determine the weight of each design objective for vehicle lift con guration and propulsion systems. The analysis consists of weighing each design objective relative to the other design objectives in order to develop a weight vector to scale scores later used in the Pugh matrix. The scoring weights for the AHP are based on the scoring system in Fig. 3.1. The results of the AHP on the vehicle lift con guration design objectives are graphically depicted in Fig. 3.2a to accompany the following discussion of the results.

Figure 3.1 AHP scoring system.

Cruise performance was determined to be the most important design objective since forward ight phases constitutes a large proportion of the mission pro le, including approximately two hours in forward ight compared to only six minutes in hover.

Hover performance was naturally the second highest factor as the vehicle needs to have reasonable hover performance in order to ful ll its role as a HSVTOL transport aircraft and complete demanding hover-oriented tasks such as those seen in VTOL CSAR roles which emphasize low DLs for the safety of ground personnel and to reduce brownout conditions.

(a) Vehicle con guration driver priority vector (b) Propulsion priority vector

Figure 3.2 Priority vectors generated by the AHP

Closely following hover performance is the maneuverability of the vehicle necessary for operations in highly contested and potentially hostile environments, especially during the high-speed penetration phase of the mission. The vehicle is in a higher threat state and thus may need to perform evasive maneuvers or normal ight to reduce detection.

The three following objectives in priority form a cluster of very close scores even though each are rather di erent in scope. Due to the competing roles of the vehicle as seen in the two highest priority objectives, cruise and hover performance, the vehicle should be able to balance these roles well and a factor is needed to encapsulate this balance. The adaptability of the vehicle is thus not an insigni cant role of the vehicle as poor performance in either task contributes to poor performance of the entire vehicle. Reducing structural complexity is essential to the vehicle's ability to achieve the above objectives as not only is high weight or bulk (parasitic drag) a detriment to performance, poor mass distribution hinders the vehicle from being able to maneuver e ectively, either preventing the vehicle from evading threats, or being unable to follow terrain closely, reducing the e ectiveness of NOE ight. Due to the harsh environments implied by the RFP, considerations must be taken to ensure that the vehicle is not overly susceptible to its environment, in particular, the vehicle will not be able to perform its mission if its propulsion system is damaged due to FOD ingestion, thus yielding a higher AHP ranking of environmental susceptibility.

It is unlikely that every design objective is of equal importance and thus even though they are still important objectives, the last two design objectives in our priority vector were mission readiness and system complexity. While they are critical to the longevity of the vehicle, they have a less signi cant direct impact on the vehicle's performance of the mission. The mission readiness of the vehicle often constitutes serviceability and reliability of components which are important factors in the lifetime of the vehicle and ultimately a system that cannot reliably accomplish its mission still fails its mission, thus they are not insigni cant to the point of dismissal, but being able to complete the mission in the rst place at all should take precedence. Similarly, system complexity deals with important factors such as the elegance of the solution, and while important, demanding challenges may result in more complex solutions.

3.2 Con gurations Considered

Brief descriptions of each con guration considered, with their qualitative advantages and disadvantages, are next described. To reduce the space requirements for these descriptions, di erent rotor con gurations (SMR, multiple rotors, coaxial) for the concepts are not broken out as the advantages and disadvantages of the di erent rotor con gurations are similar.

- Multirotor (three or more separated rotors that provide both lift and propulsion): A multirotor allows for the distribution of thrust across multiple smaller rotors, thereby permitting a smaller rotor disk area for each rotor for the same disk loading. O set placement of rotors relative to the center of gravity also allows moment control of the vehicle without the use of swashplates, although collective pitch control is still largely recommended for larger vehicles. However, due to the need to tilt the entire vehicle in forward ight to have a propulsive force, this con guration encounters severe

Figure 3.3 Con gurations considered (from top to bottom, then left to right: from Refs. 7 22)

parasite drag at higher speeds.

- Single Main Rotor (one main rotor for lift and propulsion and one tail rotor for anti-torque): Conventional single main rotor (SMR) designs are proven concepts that operate e ciently in hover and have moderate speed performance. However higher speed ight is limited by multiple physics such as the high compressibility drag e ects of the advancing blade and the stall e ects of the retreating blade. These limitations, along with diminishing power with altitude of turboshaft engines, prohibits high speed cruise at the higher altitudes design point.

- Coaxial Rotor (two vertically separated counter-rotating rotors for both lift and propulsion): The coaxial rotor has much of the SMR advantages in hover whilst reducing the vulnerability of the anti-torque device to damage or loss in e ectiveness by having counter-rotating rotors. Retreating blade e ects can also be e ectively mitigated with counter-rotating concepts although advancing blade compressibility e ects remain. The large hub structure associated with coaxial systems present a heavy drag penalty at higher speeds as well.

- Side-by-side Rotor (two horizontally separated counter-rotating rotors for both lift and propulsion): Side-by-side rotors are actually a speci c subset of multirotors and will be considered as such moving forward, side-by-side rotors are relatively large rotors with better hover e ciency whilst having less direct rotor interactional e ects as compared to coaxial rotors. They also have the bene t of providing moment control with limited cyclic control compared to SMR or coaxial con gurations. At higher speeds, tandem rotors bene t from the reduction in retreating blade e ects but su er from similar losses as multirotors in the large drag penalty as AoA increases.

- Tilt-Rotor (two or more rotors that can tilt independently, allowing the rotors to be used for both vertical lift in hover and propulsive rotors in forward ight): The tilt-rotor concept consists of a proprotor that pivots typically through a nacelle about at least one axis, typically allowing the mast axis to tilt from perpendicular to the ow in vertical ight to parallel to the ow in forward ight, allowing the rotors to act as propellers at higher ight speeds. Variations in tilt-rotor con gurations include compound tilt-fold (TF) concepts which stops and folds away the rotors at su ciently high speeds where a separate propulsor is used to propel the vehicle to higher speeds allowing where the proprotor loses e ciency. Variable diameter tilt-rotors (VDTR) area also

another high-speed variation of the tilt-rotor concept where propeller e ciency at higher speeds are increased by reducing the diameter of the proprotor at higher speeds to reduce propeller advance ratio. Conventional tilt-rotors are limited by propeller e ciency of the proprotor at high speeds due to the high propeller advance ratios and the large drag increase due to compressibility e ects as a result. High-speed tilt-rotor con gurations either marginally shift this limit as in the VDTR or have the rotor as dead weight and drag at high speeds as in the TF concept.

- Tilt-Wing (two or more rotors that can tilt with the wings for forward ight during which wings provide lift and rotors provide propulsion): Tilt-wings have proprotors xed to a pivoting wing, the primary bene t is the decreased download in hover due to the wing being slender about the axis of the rotor, however the increased weight of tilt-wing mechanisms often manifest as a disk loading penalty, the tilt-wing concept typically transitions poorly as the wing AoA is often very high as the rotor tilt increases to a point where its vertical component is a limiting factor in supporting the weight of the vehicle, thus the wing is typically stalled during the initial phases of transition.

- Intermeshing Rotor (similar to coaxial rotor con guration but the rotors are angled side-ways): The intermeshing rotor allows for a compact footprint with a similar reduction in control complexity as tandem rotors although the integrated tilt angle of the rotors reduce their e ectiveness as well as cause complicated wake interactions although the neither rotor has the disadvantage of the coaxial where the wake of one rotor may impinge upon the in ow of the other. The concept has similar drag penalties as coaxial concepts due to the large hub structure required and there is not a good means of propelling the concept to high speeds although it bene ts from the counter-rotating concept of having little to no retreating blade e ects.

- Tail-Sitter (take-o and landing on the tail, then pitches to horizontal orientation in ight): The concept consists of xed proprotor(s) mounted axially with the fuselage of the vehicle, mimicking a propeller-driven airplane. High power propulsors are needed to allow the proprotor(s) to generate su cient thrust whilst being e cient at higher speeds, as a thrust-to-weight ratio of greater than 1 would be required to hover and take-o . Challenges to the concept include maintaining su ciently low disk loadings as well as piloting the vehicle close to the ground, essentially reversing the vehicle into the ground during landing.

- Rotor-in-Wing (rotors providing both lift and propulsion are embedded in the wings): Rotor-in-wing (RIW) concepts provide compactness and low drag penalty while typically being of multirotor type, allowing for high speed ight with a thrust compounding concept, however due to the limitations of rotor size to t within the wing they typically have high disk loadings that make them infeasible for low disk loading requirements such as reduced downwash operations. The rotor systems also become susceptible to FOD damage due to the close tolerances required for e ciency of the rotors in the wing.

- Multirotor thrust and lift compounded (multirotor con guration with added wing and/or propellers for forward ight): Multirotor concept with additional lift generation at higher speeds to o oad the rotor and propulsors to propel the vehicle forward at lower angles of attack. Overcomes signi cant shortfalls in the multirotor con guration at the expense of additional weight and complexity, as foward igh speed is increased, rotors encounter the same high speed challenges, but the wing and propulsor reduces the contribution of propulsive power thus parasitic drag/power becomes the largest contributor to the high speed limit. This is further reduced by slowing or stopping the rotors as will be discussed later.

- Slowed Rotors: The slowed rotor concept reduces the advancing blade compressibility drag encountered at the drag divergence Mach number; however it does not address the asymmetric lift distribution across the retreating and advancing side, contributing to retreating blade stall. Instead a xed wing is used to augment the rotor lift at high speeds to o oad the rotor lift requirement. Conventional gearbox-driven slowed rotor drives require multiple speed ratios (at least two) which often increase weight, size, and adds more modes of failure to the system. The gearbox torque also tends to become a limiting factor in the form of the lower speeds causing an increase in gearbox torque due to the lower

rotational speed. Countertorque may still be required for some rotor con gurations in the form of a tail rotor or di erential thrust propellers in hover, which can reduce hover e ciency in comparison to other con gurations.

- Stopped Rotors: Stopped rotor concepts reduce the complexity of having a slowed rotor by removing power from the rotor, putting the rotor in autorotative state, and braking the rotor to stop it, often at a particular azimuthal orientation. The bene t of stopping the rotor is the reduction induced rotor drag, though parasite drag, dependent on the azimuthal orientation, will occur. Limitations include the azimuthal orientation of the rotor, number of blades, and increased weight and complexity of having a mechanism to clock the orientation of the rotor in an appropriate position. The con guration necessitates lift and thrust compounding due to the rotor being unable to produce useful lift when stopped. The stopped rotor remains in the ow and is subject to turbulent wakes and aeroelastic e ects.

- Stowed Rotor-in-Wing: RIW concept with shrouds to cover the rotors at higher speeds, requires thrust compounding (lift compounding is already inherent to the concept) to propel the vehicle at higher speeds. Increases the wing e ciency at high speeds due to the wing surface being uninterrupted, although RIW limitations apply, particularly in the rotor size with respect to the wing. Best suited for large wing vehicles such as blended wing vehicles.

- Stowed Open Rotors: These concepts include either a fairing that shrouds the rotor(s) or retract the rotor(s) retract into the body of the vehicle once stopped during high speed ight. Thrust and lift compounding is necessary to provide lift once the rotor is stowed. Requires a clocking and locking mechanism for the rotor system as well as actuators for either moving the rotor once stopped or to move shrouds over the rotor. Streamlines the rotor system to reduce vehicle drag although the most e ective concept is to retract the rotor which requires extremely complex actuators that would increase weight and reduce mechanical reliability.

- Reverse Velocity Rotor (RVR): The Reverse Velocity Rotor (RVR) is based on the Sikorsky RVR concept which makes use of double-ended airfoils with blunt TEs to manage the lateral rotor lift distribution at high advance ratios, in particular where the retreating blade encounters reverse ow due to the high ight speeds. The concept is similar to a slowed rotor with individual blade control (IBC) to control the blade pitch angle independent of conventional swashplate cyclic control, allowing the rotor to be controlled in hover as a conventional helicopter and in high advance ratio forward ight in a di erent control scheme to maintain controllability of the aircraft when the retreating blade is in reverse ow. Since the rotors remain spinning at high speeds, high advance ratio vibrational challenges have to be overcome and the rotor generates a signi cant portion of the vehicle's lift, thus bounding the upper limit of the ight envelope with the thrust that the rotor can generate both in lifting the vehicle as well as propelling the vehicle. Thrust and lift compounding solves this challenge although the rotor still accounts for a signi cant amount of high speed drag and the rotor is still power limited by the speed of the advancing blade.

3.2.1 Pugh Matrix

Pugh matrices were used to rank alternatives against each other with a known baseline, applying the weighting system depicted in Fig. 3.4. As the tilt-rotor con guration is the most viable currently existing con guration in operation, it was used as a baseline for the conceptual Pugh matrix.

Figure 3.4 Pugh matrix weighting system.

Figure 3.5 Vehicle lift con guration Pugh matrix scores.

3.3 Vehicle Concept Trade Study

3.3.1 Preliminary Vehicle Con gurations

Due to the high scores of the perpendicularly stopped rotor con gurations as well as the lack of precedence of such con gurations, concept sketches of the vehicle were made in order to better visualize the con guration as well as any potential issues that may arise from such con gurations.

Perpendicularly Stopped Tandem Rotor

Figure 3.6 Stopped tandem rotor concept sketches

The stopped tandem rotor con guration requires the use of double-ended airfoils as there is no convenient way to stow the rotors out of the ow. The SMR analog of the concept, the Boeing X-50 Dragon y shown in Figure 3.7a was unable to successfully transition into forward ight and the challenges of transitioning the vehicle were strongly considered, which would have required large wings and control surfaces. Most prior concepts in similar con gurations relied on the use of tip jets to augment the performance of the already large rotor(s) Room for ducting was necessary, although the nal con guration was conventionally shaft driven.

The side-by-side rotor con guration while successful in itself also produces signi cant challenges in packaging. Most designs consist of large rotors in close proximity to one another, so that the rotor disks often

(a) Boeing X-50 Dragon y Concept [23]

(b) Boeing-Vertol BV-347 with wing rotated to reduce download [24]

Figure 3.7 The stopped tandem con guration blends features from some legacy con gurations

overlap. This requires synchronized and azimuth angle o set rotors so that with rotor ap and perturbations to the tip path plane, the rotor blades do not collide. Alternatively smaller rotors with higher DL are needed.

When combined with xed wings, the concept can encounter high download if both the fuselage and the wings are in the rotorwash. The download of the wing may be minimized through the use of a tilting wing mechanism similar to the BV-347 vehicle concept (Fig. 3.7b). The addition of a tiltwing signi cantly increases the weight and complexity of the vehicle.

Perpendicularly Stopped Side-By-Side Rotor

Figure 3.8 Stopped side-by-side rotor concept sketch

The side-by-side birotor concept allows conventional airfoils to be used on the rotors when combined with partially stowing the rotor in the form of retracting the retreating blade into the main wing. A signi cant challenge of this concept would be having a large enough wing section to allow the rotor blade to be stored inside of the wing whilst balancing drag reduction methods to allow for e cient high speed cruise. This concept is most e ective when combined with two axes of rotor tilt motion, laterally for lateral control and to stow the rotors, and longitudinal for longitudinal control and low speed propulsive force until transition occurs. The concept blends the relatively large rotors of a side-by-side concept with the useful lift contribution of the rotors as wings of the stopped rotor, without the compromise of a double-ended airfoil.

This concept, in its simplest form, requires a single blade. However, when analyzed using rudimentary momentum and blade element theory (See Leishman [25]) even when employing an optimal rotor blade design, a single-bladed rotor is not capable to lift the required vehicle weight. Additionally, single-blade rotor designs require a counter balance, as there is no inherent aerodynamic balance of the rotor, leading to large oscillatory loads especially with increasing advance ratio. As such, the concept of a single-blade con guration was discarded in favor of a stowable rotor.

Past challenges to stowed rotor con gurations came in the form of either having a large shroud to streamline the xed exposed rotor, which marginally reduced the drag of the vehicle [26], or required complex mechanisms to fold the rotor into the fuselage or pylon. Prior analyses indicate that the folding mechanisms either compromised stability of the mechanism or weight of the mechanism [27]. Instead, a novel approach

was developed where stowing the rotors occurs by tilting the rotors so that they are coincident with (and stored within) the wing during high-speed ight mode. Conversely, when needed for rotorcraft mode, the rotors are tilted out of the wing-plane, providing an elegant, stable, and reliable transitional mechanism. The compromise in increased wing size can be reduced by careful airfoil choice, such as the use of supercritical airfoils, with large uniform thickness before the storage or cove region.

The tilt mechanism itself applies technology similar to extant tiltrotors, albeit over a smaller range of motion. In addition, as the rotors are designed and optimized primarily for axial operations (as compared to proprotors with large twist), larger main wing sweep angles to be employed without risk of the rotor blade-wing collisions. The sweep, along with judicious selection of transonic airfoils, will delaying the onset of drag divergence during high-speed cruise transonic ight.

Perpendicularly Stopped Quad-Rotor

(a) Early concept sketch (b) Preliminary CAD model

Figure 3.9 Stopped quadrotor concept

The quadrotor concept allows similar bene ts to the side-by-side by stowing the retreating blade into the rotor arms (or wings). While the concept is capable of potentially smaller packaging due to the lower thrust loading of each rotor, thus allowing smaller rotor sizes for the same equivalent disk loading, a caveat of the smaller size is that larger proportion of the wing/arm is required to store the rotors. These can exacerbate transition when the main wing upper surface is disrupted during rotor blade stowage. This scenario makes the concept less suitable due to the proportionally increasing thrust and reducing power to the rotors by the convertible engine concept during transition, as part of the turbofan's thrust vector would be pointing downward, against the rotor's upward thrust. Further complicating this, the di erential fore-aft collective pitch of the rotors for longitudinal pitching moments and the nose-down attitude needed to accelerate the vehicle to transition speed, forcing transition to be a more abrupt conversion in comparison to the side-by-side rotor.

3.4 Preliminary Vehicle Sizing

Due to the unique con guration of the vehicle, sizing e orts consisted of a parametric sweep of overall vehicle con gurations. Then, the performance of each vehicle con guration was estimated for rotorcraft and xed-wing modes. Gross weight variations were incorporated to con rm and de ne the mission pro le. The xed wing con gurations were analyzed rst to de ne the necessary wing extension comprised of the stopped rotor blade. For con gurations that met the cruise performance requirements, then the corresponding rotorcraft con guration was analyzed to ensure that the rotorcraft mode requirements were met. Using an estimate of operating empty gross weight (OEW) and the initial guess of the gross weight, the pool of con- gurations were then evaluated through a virtual mission pro le. For the subset that met the mission pro le requirements xed-point iterations over the fuel weight re ned the vehicle con guration converged to its optimal gross weight. The nal feasible con gurations were then ranked using various performance metrics developed from the AHP analysis to re ne their nal characteristics and select the optimal con guration. A owchart of the preliminary sizing tool is provided in Fig. 3.11.

Con dence in the team's methodologies and programming was bolstered as the results of the sizing process

are somewhat similar to study funded by NASA Ames Research Center (ARC) [1] in October of 1991 for a tilt-fold aircraft concept with a 450 KTAS (833.4 km/hr) cruise speed, 15,000 ft (4572 m) cruise altitude and 6,000 lbs (2721.6 kg mass) payload. That vehicle design had a gross weight of approximately 52,000-55,000 lbs (23,587 24,948 kg mass) and a wingspan of approximately 80 ft (24.4 m). This con guration (Fig. 3.10) was chosen as the baseline from which to compare the performance of the Harpy vehicle. The baseline con guration's mission gross weight of 57,165 lbs (25,930 kg) was within 1000 lbs (454 kg), indicating validity of the team's sizing method. More modern rotor blade designs were applied to Harpy so that some of the rotor design limitations of the earlier tilt-rotor are no longer as restrictive.

Figure 3.10 NASA ARC high-speed rotorcraft 1991 tilt-fold design used as the baseline con guration [1]

Momentum Theory (MT) equations [25] were applied in the preliminary sizing script to expedite the results as well as to obtain dimensions and weights for more re ned analysis. Fixed-wing performance equations were applied to ensure the vehicle was operating under optimal conditions during the cruise portions of the mission [28 30].

3.5 Preliminary Vehicle Con guration

The merits of the stopped side-by-side rotor concept outweighed that of the stopped tandem and stopped quadrotor concepts. The retreating blade stows into the wing, so that the rotors elegantly integrate into the main xed wing of the vehicle for high-speed forward ight.

The nal design incorporates rotors with two axes of tilt: a lateral tilt about the lateral axis to stow the rotors in the wing, and longitudinal tilt for pitch control, as well as propulsive force in low-speed forward ight prior to transition.

The con guration of Harpy permits both vertical and conventional take-o and landing operations. For the mission outlined in the RFP, the vehicle begins with unstowed rotors. The rotors are spooled up to operating RPM, and collective pitch is added to the rotor to allow the vehicle to take o vertically and hover.

The vehicle then accelerates to transition speed, where the rotor power is disengaged and begins to move into autorotative state. Once the rotor speed has slowed to an precomputed speed, the rotor brake is applied to stop the rotor. The rotor clocking mechanism is then engaged to align the rotor blades in the correct orientation for stowing. Due to the associated lift losses with the opening in the wing for storage of the rotor, the vehicle is accelerated further in this stopped con guration until the stopped rotors and xed wings are producing the lift necessary to support the vehicle's weight. During transition, the vehicle will slow due to the dynamically moving storage, to a nal speed when the transition is complete and operations are in xed-wing mode.

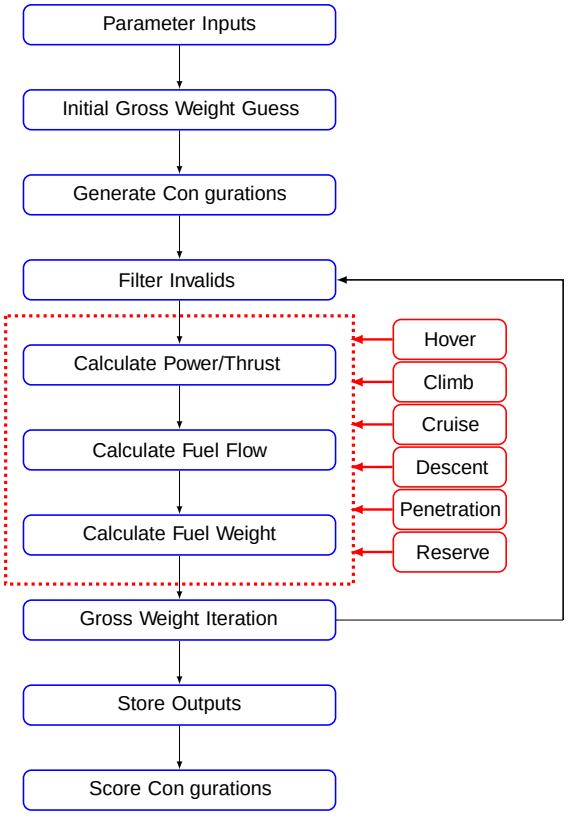

Figure 3.11 Sizing owchart

Figure 3.12 Finalized vehicle con guration of Harpy.

4 Analysis Tools

4.1 MATLAB R2022b

The team employed MATLAB extensively to write scripts and functions to size the vehicle appropriately as well as to evaluate the vehicle's performance using numerical methods and analytical solutions. The team also wrote MATLAB codes to provide numerical solutions to Blade Element (BET) and Blade Element Momentum Theory (BEMT) using the relevant equations from Leishman [25] and Johnson [31] to analyze and design the rotor blades in addition to the rotorcraft performance and stability and control.

4.2 BET/BEMT

The BET/BEMT code developed in-house was validated against experimental data [32] seen in Figure 4.1 using the SMR con guration with the high tip speed and two-bladed untwisted test con guration. This most closely matches our own blade con guration due to the low twist angle on the rotor blades and the two-blade con guration for the stowed & stopped rotor concept. The code matches the experimental data well, although as to be expected, the experimental data has slightly lower values for FM due to more complex physics not captured by the quick numerical solution a orded by BET/BEMT equations.

(a) C_T vs C_Q (b) C_T vs FM

Figure 4.1 BEMT validation against experimental data

To more accurately account for the rotor physics, the code includes corrections for both root and tip losses using the Prandtl tip loss correction factor outlined in Leishman [25].

4.3 XFOIL 6.99

XFOIL [33] is a low delity analysis tool developed by Mark Drela of MIT for quick analysis of two-dimensional airfoil sections with a focus on low Reynolds number applications. It is able to provide reasonable estimates for conditions where the ow remains attached at higher Reynolds numbers and high subsonic speeds through the Karman-Tsien compressibility correction implemented in the tool.

4.4 Solidworks 2022-2023

Solidworks [34] is a Computer Aided Design (CAD) tool further developed into a small engineering suite which provides reasonable results for basic Finite Element Analysis (FEA).

4.5 OpenVSP

OpenVSP [35] is an open-source aircraft geometry tool developed by NASA. This tool permits the parametric development of the vehicles by providing standard geometries and shapes for common aircraft parts; airfoil, wings, fuselage, propellers, etc, allowing for quick development of the vehicle design by simply changing various parameters, as required. The software provides other sub-tools such as the parasite drag tool to determine the drag breakdown of the vehicle. The Vortex Lattice Method (VLM) was employed to perform stability analysis. As potential-based tools do not include viscous drag, the Blasius and Schlicting compressible equations were provided the laminar and turbulent equations, respectively, with which viscous drag effects were estimated.

5 Vehicle Design Overview

The final Harpy vehicle was sized using the method outlined in Section 3.4. This section provides an overview of the final vehicle design for reference, and the remainder of the report furnishes more of the details that resulted in the final design. A three-view drawing of the vehicle in fixed-wing mode, with dimensions, is included on the following page. A second three-view drawing illustrates the vehicle in rotorcraft mode. Following these is Table 5.1 that provides a detailed breakdown of the Harpy dimensions.

The representative power and thrust curves at SDGW for these two operational modes of Harpy are depicted in Fig. 5.1. Conversion of Harpy from rotorcraft to fixed-wing mode is twofold: first Harpy is accelerated with flaps deflected 25 to the stopped rotor speed where the rotor-wing and main wing system is capable of generating sufficient lift to support the vehicle at SDGW. Acceleration is initiated by longitudinal nacelle tilt and as forward flight speed increases, which reduces the power requirements of the rotor as wing lift increases, the convertible engines proportionally increase thrust and reduce torque output to maximize acceleration speed. At stopped rotor speed, the rotors are disengaged, Harpy's rotors move into autorotative state and are brought to a stop via a rotor brake. Once stopped, the rotors are moved into the fixed-wing orientation in preparation for integration with the main wing.

Next, to anticipate the partial loss of main wing lift when the sliding doors open the rotor storage cavity, Harpy accelerates further to the transition speed. At this speed, the wing is capable of generating sufficient lift at the SDGW even when the rotor storage cavity is open. The already stopped rotors are then retracted into the main wing out of the flow and the conversion is complete.

Figure 5.1 Harpy power and thrust curves

Harpy	Dimensions in ft and (m)				
Wing, Rotor, Empennage	Wing	Wing+Rotor	H. Stab.	V. Fin	Rotor
Area: Theoret.|Disk	840.5 (78.1)	1,056.5 (98.2)	370 (34.4)	216 (20.1)	1018 (94.6)
Area: Exposed|Blade	673.7 (205.3)	832.1 (253.6)	190.6 (58.1)	216 (65.8)	108 (10.03)
Span: Overall|# Blades	52.6 (16.03)	100 (30.5)	37 (11.3)	13.5 (4.11)	2 (0.61)
Span: Exposed /Side|Radius	20.33 (6.2)	44 (13.4)	13.65 (4.2)	13.5 (4.11)	18 (5.5)
Sweep Angle (deg)	20	20	25	25	Parabolic
Dihedral/Cant Angle (deg)	3	3	0	0	17
Root: Theoret. Chord	16 (4.9)	16 (4.9)	10 (3.05)	10 (3.05)	6 (1.8)
Root: Max Thickness	2.88 (0.88)	2.88 (0.88)	1.2 (0.37)	1.2 (0.37)	0.57 (0.17)
Tip: Theoret. Chord	11 (3.4)	6 (1.8)	10 (3.05)	10 (3.05)	0 (0)
Tip: Max Thickness	1.98 (0.6)	0.57 (0.17)	1.2 (0.37)	1.2 (0.37)	0 (0)
Aspect Ratio	11.90	9.47	3.7	1.69	3
Taper Ratio	0.688	0.375	1	1	Parabolic
Ctrl. Surf.: Wing	TE Flaperons	Rotor-Ailerons			
Area	48.55 (4.51)	108 (10.03)			
Ctrl. Surf.: Fuselage	Elevator	Rudder	Windshield		
Area	111 (10.3)	46.7 (4.34)	96.49 (8.96)		
Rotor Artic. & Tip Speeds	Type of Artic.	Tip Speed			
	Hingeless	780 ft/s (237.7 m/s)			
Fuselage	Length	Max Depth	Max Width	Surf. Area	Volume
	82.5 (25.1)	12 (3.66)	15 (4.57)	2,816.8 (261.7)	7,956.6 (225.3)
Alighting Gear	Max. Length	Oleo Travel	Vert. Stroke		
	2.5 (0.76)	1.5 (0.46)	1.5 (0.46)		
Air Induction	Capture Area	Circum.@Engine	Duct Length		
	7.5 (0.7)	12 (3.66)	19 (5.79)		
Propulsion	Continuous				
	Rating	RPM			
Power	8,000 hp (5,965.6 kW)	7,400			
Thrust	15,000 hp (11,185.5 kW)	7,400			
Fluid Cap.	Protected				
Fuel Sys. (Fuselage)	Cells	Tot. Gals.			
Internal	1	2,445 (9,255.3 L)			
Oil Sys.	1	25 (94.6 L)			

Table 5.1 Harpy dimensional data

Although Harpy does not typically operate in rotorcraft mode beyond its transition speed, the rotor power curve was extended to twice the transition speed to provide a better visual representation of the curve. Due to the use of supercritical airfoils and a moderate amount of sweep, the onset of drag divergence

due to Mach is delayed and the thrust curves has a large area of speed stability, allowing Harpy to cruise efficiently over a large range of high speeds. This is apparent in the shape of the curve when compared to the projected tangent line indicating the best range speed. At 20,000 ft (6096 m) ISA conditions, Harpy's drag does not significantly increase until 500 KTAS (257 m/s) allowing Harpy to be capable of maximum level flight speeds in excess of 540 KTAS (278 m/s).

Figure 5.2 Footprint overlay comparison between the Harpy and the Chinook.

Shown in Figure 5.2 is a full-scale footprint overlay of the Harpy. While the Harpy's lateral footprint is larger in comparison to the Chinook, it should be noted that its longitudinal footprint is smaller, putting the Harpy at comparable sizes to in-use VTOL vehicles. This allows the Harpy to access the same areas the Chinook can.

5.1 Vehicle Mission Performance

The mission breakdown is displayed in Tables 5.2 5.3. The climb phase was parsed into additional intermediate climb segments to include the conversion of Harpy (as outlined in the prior subsection) as the transition segment. The transition phase of the mission highlights the use of the convertible engine. The engine utilization is maximized to extract as much of the thrust available for acceleration while maintaining level flight. It should be noted that power and thrust available in this context refers to 90% of maximum continuous power rating, thus satisfying the RFP requirement of not exceeding 100% P_{mcp} for any segment and 90% P_{mcp} at MMGW.

Due to the limited space, duplicate segments are grouped together with outbound and inbound denoting the initial and repeated segments respectively.

Flight Idle		
Pressure Altitude	2,000 ft (609.6 m)	
Ambient Temperature	85 F (29.4 C)	
Avg. Gross Weight	51,316 lbs (23,276.5 kg)	
Airspeed	0	
Segment Characteristics	10 min	
Fuel Flow	909.83 lbs/hr (412.69 kg/hr)	
Power Required	Idle	
Power Available	12,750 hp (9378 kW)	
HIGE		
Pressure Altitude	2,000 ft (609.6 m)	
Ambient Temperature	85 F (29.4 C)	
Avg. Gross Weight	50,125 lbs (22,736 kg)	
Airspeed	0	
Segment Characteristics	2 min	
Fuel Flow	3,850.5 lbs/hr (1,746.6 kg/hr)	
Power Required	9,923 hp (7,400 kW)	
Power Available	12,750 hp (9,378 kW)	
Transition	Outbound	Inbound
Pressure Altitude	2,000 ft (609.6 m)	
Ambient Temperature	85 F (29.4 C)	
Avg. Gross Weight	51,138 lbs (23,195 kg)	43,156 lbs (19,575 kg)
Airspeed	123 KTAS (227 km/h)	113 KTAS (209 km/h)
Segment Characteristics	0.85 nm (1.57 km)	0.53 nm (0.97 km)
Fuel Flow	14,342 lbs/hr (6,505 kg/hr)	14,793 lbs/hr (6,710 kg/hr)
Power Required	4,421 hp (3,297 kW)	3,564 hp (2,658 kW)
Power Available	4,421 hp (3,297 kW)	3,564 hp (2,658 kW)
Thrust Required	16,828 lbs (75 kN)	18,051 lbs (75 kN)
Thrust Available	16,828 lbs (75 kN)	18,051 lbs (75 kN)
Accelerate to Climb	Outbound	Inbound
Pressure Altitude	2,000 ft (609.6 m)	
Ambient Temperature	85 F (29.4 C)	
Avg. Gross Weight	51,010 lbs (23,138 kg)	43,055 lbs (19,529 kg)
Airspeed	220 KTAS (407 km/h)	220 KTAS (407 km/h)
Segment Characteristics	1.72 nm (3.19 km)	1.45 nm (2.65 km)
Fuel Flow	19,972 lbs/hr (9,059 kg/hr)	19,972 lbs/hr (9,059 kg/hr)
Thrust Required	23,906 lbs (106 kN)	23,906 lbs (106 kN)
Thrust Available	23,906 lbs (106 kN)	23,906 lbs (106 kN)
Climb	Outbound	Inbound
Pressure Altitude	2,000+ ft (609.6+ m)	
Ambient Temperature	51.87 F (11.04 C)	
Avg. Gross Weight	40,471 lbs (18,357 kg)	42,587 lbs (19,317 kg)
Airspeed	220 KTAS (407 km/h)	220 KTAS (407 km/h)
Climb Speed	3,000 ft/min (914 m/min)	3,000 ft/min (914 m/min)
Segment Characteristics	24.44 nm (45.26 km)	24.44 nm (45.26 km)
Fuel Flow	8,272.2 lbs/hr (3,752.2 kg/hr)	7,235.9 lbs/hr (3,282.1 kg/hr)
Thrust Required	10,148 lbs (45 kN)	8,876.2 lbs (39.48 kN)
Thrust Available	25,455 lbs (113 kN)	25,455 lbs (113 kN)

Table 5.2 Vehicle mission metrics.

Cruise	Outbound	Inbound
Pressure Altitude	20,000 ft (6,096 m)	
Ambient Temperature	-12.32 F (-24.62 C)	
Avg. Gross Weight	46,374 lbs (21,035 kg)	39,133 lbs (17,750 kg)
Airspeed	450 KTAS (833.4 km/h)	450 KTAS (833.4 km/h)
Segment Characteristics	405.3 nm (750.6 km)	408.8 nm (757.1 km)
Fuel Flow	5,802.6 lbs/hr (2,632 kg/hr)	5,721.1 lbs/hr (2,595 kg/hr)
Thrust Required	6,034 lbs (26.77 kN)	5,949 lbs (26.44 kN)
Thrust Available	14,388 lbs (64.00 kN)	14,388 lbs (64.00 kN)
Descent	Outbound	Inbound
Pressure Altitude	20,000 ft (6,096 m)	
Ambient Temperature	-12.32 F (-24.62 C)	
Avg. Gross Weight	44,185 lbs (20,042 kg)	36,647 lbs (16,623 kg)
Airspeed	77.21 KTAS (143 km/h)	220 KTAS (207 km/h)
Descent Speed	3,000 ft/min (914 m/min)	3,000 ft/min (914 m/min)
Segment Characteristics	6.7 min	6.7 min
Fuel Flow	1,027.6 lbs/hr (466.1 kg/hr)	1,027.6 lbs/hr (466.1 kg/hr)
Thrust Required	0 lbs (0 kN)	0 lbs (0 kN)
Thrust Available	14,388 lbs (64.00 kN)	14,388 lbs (64.00 kN)
Penetration	Outbound	Inbound
Pressure Altitude	2,000 ft (609.6 m)	
Ambient Temperature	85 F (29.4 C)	
Avg. Gross Weight	43,702 lbs (19,823 kg)	35,994 lbs (16,326.6 kg)
Airspeed	540 KTAS (1,000 km/h)	540 KTAS (1,000 km/h)
Segment Characteristics	50 nm (92.6 km)	50 nm (92.6 km)
Fuel Flow	26,217 lbs/hr (11,892 kg/hr)	26,217 lbs/hr (11.892 kg/hr)
Thrust Required	23,906 lbs (106 kN)	23,906 lbs (106 kN)
Thrust Available	23,906 lbs (106 kN)	23,906 lbs (106 kN)
HOGE	Outbound	Inbound
Pressure Altitude	2,000 ft (609.6 m)	
Ambient Temperature	85 F (29.4 C)	
Avg. Gross Weight	43,233 lbs (19,610 kg)	35,536 lbs (16,119 kg)
Airspeed	0	0
Segment Characteristics	2 min	2 min
Fuel Flow	2,543.2 lbs/hr (1,153.6 kg/hr)	1,931.4 lbs/hr (876.05 kg/hr)
Power Required	6,787 hp (5,061 kW)	5,245 hp (3,911 kW)
Power Available	12,750 hp (9508 kW)	12,750 hp (9508 kW)
Reserves		
Pressure Altitude	2,000 ft (609.6 m)	
Ambient Temperature	85 F (29.4 C)	
Avg. Gross Weight	35,240 lbs (15,985 kg)	
Airspeed	146.9 KTAS (272 km/h)	
Segment Characteristics	48.97 nm (3.14 km)	
Fuel Flow	1,580.3 lbs/hr (716.8 kg/hr)	
Thrust Required	2,037 lbs (9.1 kN)	
Thrust Available	23,906 lbs (106.3 kN)	

Table 5.3 Vehicle mission metrics continued.

5.2 Vehicle Systems Overview

5.2.1 Vehicle Performance Data

Harpy's performance characteristics are summarized in Table 5.4 and associated performance plots are displayed in Figures 5.3 5.4.

Characteristic	English Units	SI Units
Hover ceiling	10,791 ft	3,289 m
Service ceiling (rotor)	27,688 ft	8,439 m
Service ceiling (xed-wing)	51,600 ft	15,750 m
Max dynamic pressure	455 psf	21,800 N/m^2
Max level ight speed	540 KTAS	1,000 km/h
Best range speed	292 KTAS	541 km/h
Best climb speed	220 KTAS	407 km/h

Table 5.4 Vehicle performance metrics.

(a) Hover ceiling

(b) Rotor service ceiling

(c) Rotor equivalent lift to drag up to 150 KTAS

Figure 5.3 Harpy rotorcraft mode performance at SDGW

(a) Service ceiling (b) Velocity-load factor diagram

Figure 5.4 Harpy xed-wing mode performance at SDGW

5.2.2 Vehicle Control Systems

The vehicle control systems are provided in Table 5.5. SinceHarpy's rotors have two axes of tilt, an additional mode of control in rotor-modes not feasible in other VTOL con gurations, lateral translation without roll moment, this is made possible by the lateral gimbal tilt of the rotors. The ability to do so makes Harpy particularly suited for CSAR operations were ne control may be needed without disrupting a winch through rolling motion.

Flight Con g	Torque Bal	Long. Pit	Lat. Roll	Vert. Motion	Directional
Hover Rotor-Edgewise	Counter-rotating	Nacelle tilt (longitudinal)	Rotor di collective	Rotor collective	Nacelle di tilt (longitudinal)
Transition Fwd Flight	No torque	Elevator de ection	Rotor-ron de ection	Thust increase	Rudder de ection

Table 5.5 Vehicle Control System

6 Aerodynamic Design

Harpy was designed with a large emphasis on maximizing cruise performance. Once the vehicle was sized for the mission, drag reduction measures in high subsonic regime were identi ed as key to minimize wave drag e ects for e cient cruise in the transonic regime. Supercritical airfoils for the main wing section were explored, along with the application of Whitcomb's [36] area rule to the fuselage cross-section. The supercritical airfoil not only permits better transonic performance but also provided the necessary internal volume for the storage of the rotor system when the retreating blade is stowed into the wing.

6.1 Fuselage Outer Mold Line Design

The fuselage was designed to meet the cargo requirements , but it also needs to be aerodynamically e cient, in particular at the high-speed cruise condition. In order to minimize drag, the transonic area rule was incorporated into the design of the fuselage outer mold line. In particular, the nose and main sections were altered to address this. Instead of a constant elliptical shape throughout the entire length of the main section, the width and height of the cross sections were optimized to minimize the change in area as much as

possible while still maintaining structural and payload requirements. The cross sectional area of the vehicle in forward flight configuration as a function of fuselage longitudinal axis (x-position) is shown in Fig, 6.1.

Figure 6.1 Harpy cross-section distribution with application of area rule.

The alterations in the fuselage cross section were primarily to mitigate a significant and abrupt change in the fuselage cross-sectional area between 10 ft and 25 ft. The fuselage in this region was smoothed, as shown in the figure, reducing the wave drag that was present.

6.2 Airfoil Selection

A number of different airfoils were evaluated to determine which extant airfoils would be best suited for the rotor, wing and tail surfaces. New bespoke airfoils were not designed, rather the components were designed from the best airfoils analyzed. There were different sets of airfoils for the different components. The airfoil selection was evaluated in multiple ways: using existing experimental and high- delity computational fluid dynamics data from UIUC [37], Abbott and von Doenhoff [38], papers, such as Smith et al [39], and C-81 tables already developed at Georgia Tech. These data provided insights on the airfoil characteristics at various Mach numbers and angles of attack. These were augmented by a series of XFoil simulations to extend the data available.

For the rotor, six different airfoil series were considered for the design extracted from NACA, CLARK, EPPLER, Boeing Vertol, Sikorsky and ONERA airfoil families. The SC1095, SC1094-R8, OA209, VR-13, NACA0012, and NACA0009, were final candidates for the rotor blade. The SC1095 and SC1094-R8 airfoils were selected for the rotor based on their lift-to-drag ratio and mild pitching moment response over the

proposed Mach range of the rotor. Their proven success on the Sikorsky Blackhawk helicopters was also a positive factor.

Since the cruise ight condition lies in the transonic regime, the supercritical series of airfoils were preferred due to the reduction of wave drag since the design resulted in a higher critical Mach number and Mach drag divergence due to the design of the upper surface. The relatively at upper aft surface was also a considered a positive for the rotor storage cavity on the wing. For the wing airfoil choice, the SC 20518, NACA64(3)-618, NACA23018, CLARK YM-18, and the EPPLER 1098 were evaluated, out of which the SC20518 was selected for the main wing.

The NACA-64012 was selected for the vertical tail and horizontal tail. While this is not a supercritical wing, with su cient aft sweep (25 in the nal design), the local Mach number was below the drag divergence Mach number. The nearly linear aft shape of the airfoil aided a rapid progression of the shock to the trailing edge. Cruise operation of the Harpy calls for an angle of attack within the airfoil drag bucket, which combined with its mild pitching moment variation, made it an optimal choice for the tail.

6.3 Tail Con guration

A trade study on tail con gurations was evaluated to determine the best tail design for Harpy. The trade study included the analysis of multiple tail con gurations built with the selected NACA-64012 airfoil. The tail con gurations considered, along with their advantages and disadvantages, include:

- Conventional Tail: One of the biggest advantages of the conventional tail con guration is that it is light in weight, and it requires less structural weight over other options. Since the horizontal stabilizer is near the center of gravity it reduces the bending moment, helping in weight savings. A horizontal stabilizer without separate elevators permits improved pitch control without over complicating the design. This disadvantage of this con guration is that there cannot be tail-mounted engines, which can interfere with yawing movement if the engines fail. The tail has an increased chance of wake immersion from the wing, which negatively impacts the performance and stability of the vehicle. Since the horizontal stabilizer is close to the wings, the entrained air ow over the stabilizer can lead to a potential loss of control of the pitch.

- H-Tail: There are two factors that make the H-Tail more desirable over the conventional tail. The tail con guration o ers vertical tail redundancy in case of failure mid-operation. If one of the tails is damaged, then the other vertical tail can provide stability to the vehicle. The tail con guration also o ers spin resistance which improves the vehicle's ability to resist entering and maintaining a spin. Since the con guration also has additional vertical surface area, it increases the yaw stability which makes it harder to enter spin. Since there is additional surface area and complexity in design, it increases the weight of the structure. This in turn results in additional viscous and, in some attitudes, pressure drag that can impact the overall performance. The structural supports to reinforce the extra surface area adds additional weight as well.

- Cruciform Tail: The cruciform tail has a fairly simple design and is a more commonly used design for aircraft. This familiarity further reduces any risks that may exist with complex designs. It also has less wing-induced e ects on the horizontal stabilizers. Conversely, due to the horizontal stabilizer intersection with the midspan of the vertical stabilizer, there can be more performance issues, similar to the conventional tail, dependent on where the engine is mounted.

- T-Tail: With the T-tail con guration, there is reduced interference from the wing-generated turbulence. Since the horizontal stabilizer is above the wing, it reduces the chances of the wing wake interfering with the tail. It also has reduced interference drag, improved e ciency at high speeds, increased control, and better yaw stability. The downside of the T-Tail con guration is that it is a heavy structure which adds to the overall weight of the vehicle. The structures and control system are heavier and more complex than many other tail con gurations. The T-tail can also be impacted aerodynamically due to wing wake interference at high pitch angles.

- V-Tail: For the V-tail, the best advantage is that it is very lightweight structurally as there are no horizontal or vertical stabilizers. The diagonal V-shape also reduces the weight, contributing to higher fuel e ciency. There is usually low interference drag between the tail and the wing wake due to the V-construction. There are structural issues that arise with the complexity of the design with respect to control systems to ensure proper functionality with its control surfaces. The V-tail may have increased bending and torsional stresses on the tail surfaces and experience (higher) vibratory loads during turbulent ights.

6.4 Drag Breakdown

The drag breakdown was accomplished at the cruise condition of 20,000 ft (6096 m) 450 KTAS (232 m/s) cruise condition. The dynamic pressure-normalized force and moment equivalent areas of the airframe at zero degrees of pitch and yaw summarized in Table 6.1. These values are the fuselage only, since, as required by the RFP, all lifting surfaces and rotor systems were not included, and the landing gear is retracted.

Airframe Parameter	Cruise
Lift Area ($\frac{L}{q}$)	0 ft^2
Parasite Drag Area ($\frac{D}{q}$)	24.13ft^2
Pitching Moment Volume ($\frac{M}{q}$)	-43.704ft^3
Parasite Side Force ($\frac{Y}{q}$)	0 ft^2

Table 6.1 Dynamic pressure-normalized equivalent airframe areas for cruise and nominal transition at = 0^o = 0^o.

The drag breakdown was estimated in two ways, rst using traditional methods, as described in Prouty [40] (pgs. 303-306) and using the modern OpenVSP solver. The former approach ensured that the team understands the principles and computations, while the latter approach provided what is considered to be a more accurate estimation. The parasite drag was estimated using the Blasius equation for the laminar ow and the Schlichting compressible boundary layer equation on the di erent components. The equivalent at plate drag can be more accurately estimated using the form factor for highly irregular for the components was determined from the sizing code and factored into the tool. The drag tool uses the Blasius Equation for the laminar ow equation and the Schlichting Compressible equation for the turbulent ow. Comparisons of the at plate drag areas were very close, for example within 2 ft^2 for the wing. The traditional approach typically predicted slightly higher equivalent at plate drag.

Component	F.P. Area ft^2 (m^2)	C_d	C_{d_v}	Source
Main Wing	8.19 (0.76)	0.0078	0.773	Prouty
Right Rotor	1.053 (0.098)	0.000997	0.0993	Prouty
Left Rotor	1.053 (0.098)	0.000997	0.0993	Prouty
Fuselage	8.28 (0.76)	0.0078	0.2518	Prouty
Horizontal Tail	4.53 (0.42)	0.0043	0.3403	Prouty
Right Vertical Tail	0.506 (0.047)	0.000479	0.0066	Prouty
Left Vertical Tail	0.506 (0.047)	0.000479	0.0066	Prouty
Total	24.13 (2.24)	0.0228	1.5769	

Table 6.2 Component drag buildup in forward and vertical ight at SDGW

7 Rotor Design

The rotors of Harpy were designed to keep the DL under a target maximum DL of 25 psf (1197 Pa), with a maximum wake velocity of 191 ft/s (58 m/s) or 113 KTAS (209 km/hr) [6]. As high-speed ight

performance was given highest priority, the rotor blade twist more closely matches angles seen in xed wing washout angles instead of typical rotorcraft twist angles designed for hovering and moderate advance ratios.

Harpy's rotor was designed using the BEMT code outlined in Section 4.2. Rotor size was limited by packaging in the main wing, which further constrained taper to ensure su cient solidity to remain below a blade loading coe cient stall limit of 0.12. [25] These limitations reduced the design space signi cantly which meant that every remaining design parameter was crucial to enabling Harpy to excel at its tasks.

Since Harpy operates as a rotorcraft at lower end of its forward ight speed regime (M 0:25), the hover tip speed margin of the rotors can be increased, with judicious airfoil selection to avoid compressibility e ects and noise limits (in this RFP, this impacts survivability). The design tip speed, V_{tip} was selected as 780 ft/s (238 m/s), which matches the baseline con guration [1]. This high tip speed gives Harpy a larger blade stall margin and, when coupled with the relatively small rotor radius, reduces the torque load on the transmission, allowing smaller, more lightweight transmissions, contributing to lower gross weights.

The design restrictions on twist and taper as well as material technology limitations meant that Harpy's rotor blades would largely be untapered and untwisted except for the tip sections, where twist aids to avoid higher losses, and where the highest speeds would be achieved. A future rotor design enhancement can explore morphing wing technology to twist the rotor blades to high twist angles during hover and untwist the rotor blades to low twist angles when stopped, especially given the high loads experienced by rotor blades. Morphing rotors were not considered in this design, as the team's technology development extrapolation analysis was slightly outside the RFP date guidelines.

Harpy's nal rotor design characteristics are outlined in Table 7.1 and the rotor blade is illustrated in Fig. 7.1. The nal rotor design was completed with the BET/BEMT code. Very high quality airfoil or C-81 tables, previously developed using the NASA OVERFLOW solver and advanced large eddy simulation (LES) turbulence closures, were available at Georgia Tech for the SC1095 airfoil. The linear aerodynamic portion of the C-81 tables were adjusted for the SC1094 R8 (and other airfoils evaluated during design), keeping the nonlinear regime behavior at large angles of attack consistent (with appropriate merging of the two regimes) with the SC1095 tables. The linear aerodynamic regions were computed with XFOIL per the tools description (Sec. 5). Due to page constraints, the reader is directed for further details and illustrations of the C-81 tables in Smith et al. [39].

Figure 7.1 Harpy rotor design.

The relationship of the rotor performance with respect to gross weight was explored in Figures 7.2a 7.2b using the in-house developed BEMT code. The gross weights explored varied from the vehicle empty weight to 10% over the SDGW of the vehicle. In Fig. 7.2a the upper limit of the rotor performance before being stall limited is about 55,000 lbs (244,652 N, 24,948 kg), which would indicate the rotor is capable of increasing its payload capability, particularly if an alternative mission is required that permits an initial conventional take-o at maximum gross weight.

The relationship of gross weight to Figure of Merit (FM) follows the same trend of thrust coe cient to

Characteristic	English	SI
R	18 ft	5.49 m
	0.2012	0.2012
R	780 ft/s	238 m/s
DL	25 psf	1205 N/m^2
FM	0.81	0.81
C_T =	0.1090	0.1090
P_{HOGE}	9,193 hp	6,856 kW
D_v=GW	4.76%	4.76%

Table 7.1 Hover performance characteristics from BEMT code.

(a) Gross weight vs Figure of Merit (b) Figure of Merit vs blade loading coe cient

Figure 7.2 Gross weight sweep of the Harpy rotor

Figure of Merit as observed and expected in the validation of the BEMT code.

Even though Harpy does not operate at traditional SMR high edgewise maximum speeds, the Harpy rotor blades have a parabolic taper to create a more uniform lift distribution in xed-wing mode where the tip taper is closer to an elliptical shape than a rectangular tip. In addition, this creates a more uniform in ow distribution at the rotor tips, where tip losses tend to result in higher in ow velocities. The e ects of this taper are illustrated in Figure 7.3a where the wake velocity of the Harpy rotor remains under the wake velocity limit [6] compared to an equivalent blade with untapered planform, which shows a sharp rise in in ow velocity (and hence wake velocity) at the tips. The parabolic tips have the added bene t of providing a parabolic leading edge sweep to more optimally mitigate compressibility e ects over a linear taper during high speed edgewise ight, increasing the ight envelope of rotorcraft mode.

Due to Harpy's unique conversion requirements, more sophisticated rotor tips were not implemented to avoid adverse characteristics during the xed-wing mode, where Harpy spends most of its operational time. BERP-style tips, while useful in dynamic stall conditions that arise from high speed edgewise ight, are not necessary for Harpy and only increase drag and generate non-ideal lift distributions when the rotors are stopped and acting as xed-wing components.

7.1 Rotor Hub

Since Harpy's rotors must operate both as rotary wings, where large centrifugal moments aid in balancing aero moments generated by the lift of the rotor blades, as well as xed wings, where there are no centrifugal

(a) Wake velocity of the Harpy rotor (b) Thrust coe cient distribution of the Harpy rotor

Figure 7.3 Harpy rotor blade analysis

moments to o set the lift of the wing, a highly rigid rotor hub was used to minimize aeroelastic e ects when the rotors are in the stopped con guration. With this in mind, the rotor hub consists of a large, highly rigid composite ex beam similar in construction to the Airbus Star ex or Spheri ex rotor systems, the former of which is shown in Fig. 7.4.

Figure 7.4 Airbus H130 hingeless rotor hub [2]

Such composite ex beam rotor hub designs permit aeroelastic tailoring of ap, lag, and feathering modes through sti ness modi cations. Further, the design increases the time interval between (and complexity of) maintenance due to the lack of hinges and bearings, which are more susceptible to dust and debris. The conceptual layout of the composite rotor is illustrated in Fig. 7.5.

The unique loading of the rotor system across both ight modes directs another novel design concept. That is, that both the rotor hubs and the blades make use of tailored composite layups that allow a exible rotor when an axial tensile load (centrifugal forces) is applied during rotation, but a more rigid rotor when there is no rotation. This rotor exibility provides greater stability in rotary-wing mode where perturbations are dampened by the axial loads and improve rotor structural dynamics particularly for the 1/rev modes. During xed-wing mode the tailored layup will allow the rotor to be sti er during high-speed cruise.

Figure 7.5 Harpy's rotor construction.

8 Structural Design

The structural elements of Harpy are designed to maintain airframe integrity for airworthiness even in continuous operation under adverse ight conditions. Every structural element was speci cally designed to withstand the force ampli cation of 3.5g as well as its associated airload on the component, which is re ected accordingly in the load analysis for both rotorcraft and xed wing modes. Additionally, the landing gears and the aircraft structure are designed to handle landing impacts with 2/3 of rotor lift available at a sink speed of 10 ft/s (3.05 m/s). Here, a high-level structural scheme is proposed, which includes placement and con guration of load-bearing components. The vehicle overall employs typical sheet-stringer design for both fuselage and wings.

The limit loading conditions follow the requirements outlined in the RFP [41]. The limit loads di er depending on the vehicle operation: xed-wing mode, rotorcraft mode, upon landing, and on the ground. The wing lift distribution in xed-wing mode is assumed to be elliptically distributed. All xed-wing load analysis was performed with an applied 3.5 g load factor to ensure the structure is designed su ciently. The loads on the hovering rotor blade is calculated from BEMT analysis, and then applied to the tip of the main wing's xed portion. The landing impacts are calculated and applied assuming the 10 ft/s (3.05 m/s) sink speed rate condition from the RFP.

8.1 Fuselage Load Analysis

With the loadings resolved, structural loading on the fuselage was calculated. The structural loads were analyzed at the front and aft of the main wing bulkhead, by assuming the fuselage is cantilevered and supported at the main wing bulkhead interfaces. As shown in Fig 8.1, the maximum shear force on the fuselage turns out to be around 87,500 lbs (433,700 N), and the maximum bending moment is 1,300,000 lb-ft (1,762,600 Nm), both at the wing bulkhead interface under 3.5g load factor for the xed-wing mode. The fuselage structure consists of 24-longerons and bulkheads with 20-inch spacing. The proposed fuselage structure is depicted in Fig 8.2, which includes the bulkhead and longeron placements to support 3.5g pull-up maneuver. The proposed material is aluminum 7075-T6 with optional consideration of moving towards thermoset and thermoplastic composites for increased weight e ciency. The proposed skin thickness is 0.095" (2.4 mm) with thermoplastic composite being selected as the skin material.

8.2 Wing Load Analysis

The shear force and bending moment distribution across the xed wing is calculated similar to the approach applied to the fuselage, with the stated landing condition included as well. The maximum

Figure 8.1 Fuselage shear force and bending moment distribution under di erent operating conditions

Figure 8.2 Multiple view of the fuselage structure.

Figure 8.3 Main wing shear force and bending moment distribution under di erent operating conditions

Figure 8.4 Multiple view of the wing structure.

shear force is computed to be 86,500 lbs (384,800 N) and the maximum bending moment is 1,820,000 lb-ft (2,467,600 Nm), both at the wing root, under the 3.5g load factor during xed-wing mode.

The wing employs conventional sheet-stinger structure. However, the wing structure of Harpy also has a unique requirement to accommodate the stowage of the rotor blade. A relatively thick airfoil was chosen to ensure adequate space for blade storage while retaining su cient wing cross-sectional area to accommodate the required internal structural elements. This consideration is critical to the design of Harpy since the unique design requires the main wing having to withstand signi cant load at its tips, originating from gravitational loads and thrust from the rotor system. When in rotorcraft mode, the entirety of the vehicle's gross weight is supported by the rotors, resulting in a larger bending moment at the root of the main wing. Shown in Fig 8.4, nearly half of the wing's cross-section is required for the sliding door and blade stowage. The remainder of the wing consists of webbed ribs with 18-inch spacing, 16 J-stringers, and a 3-spar construction. A 3-spar con guration is not uncommon for aircraft with high wing loads, such as Lockheed C-5 Galaxy [42], to support 3.5g pull-up maneuver.

8.3 Landing Gear

A landing gear was designed to withstand an impact under the landing condition of 2/3 of rotor lift alive, with a sink speed of 10 ft/s (3.05 m/s). A single nose gear and a twin main gear con guration was chosen and used for this analysis. The landing gear strut compression is considered to be 12 inches (30.48 cm) maximum, with a tire compression of 6 inches (15.24 cm). Under these conditions, the landing impact was estimated to be 20,800 lbs (92,523 N) for the nose gear and 41,700 lbs (185,500 N) for the main landing gears combined, su cient for the RFP requirements and this design.

8.4 Cabin Pressurization Consideration

At the cruise altitude of minimum 20,000 ft (6,100 m), a pressurized cabin sees about 3.77 psi (62.9 kPa) pressure di erence between inside and outside of the cabin, having the cabin pressurized to 8,000 ft (2,440 m). In compliance to 14 CFR 25.365 which calls for a consideration of cabin pressurization above 45,000 ft (13,720 m), an extreme case of Harpy being placed at 50,000 ft (15,240 m) was considered for pressure load analysis which ends up with 9.14 psi (0.63 bar) pressure di erence. With simple pressure vessel assumption, at an extreme pressurization case at 50,000 ft (15,240 m), the maximum hoop stress is estimated to be 8,400 psi (58 MPa) and the maximum axial stress is estimated to be 4,200 psi (29 MPa), with the previously mentioned wall thickness. As 7075 aluminum has fatigue stress of about 23,200 psi (160 MPa), the fuselage thickness selection is determined to be appropriate. Additionally, thermoset composites such as Carbon Fiber Reinforced Plastics (CFRP) can be utilized as it has fatigue stress able to reach 43,500 psi (300 MPa), depending on the ber orientation and layup.

9 Powerplant System

9.1 Engine Con guration Determination

Given the possible design space, there were a variety of possible powerplant con gurations. However, due to the heavy emphasis on propulsion performance and long range, many alternatives such as full electric power and hydrogen power became infeasible due to propulsion weight and size. Additionally, electric hybrid power lacked su cient bene ts to validate the increase in system complexity, thus it was determined that turbomachinery would be the most appropriate propulsion system for Harpy.

Turbojets, turbofans, and turboshafts were amongst the turbomachinery con gurations were considered during the trade study. While turbojets o er great performance ceilings, their relative lack of e ciency compared to turbofans and the subsonic mission pro le meant that turbofans were chosen for Harpy.

To drive the rotors, either a set of turboshaft engines or a convertible turbofan engine as discussed in

Section 9.4.1 would be needed. To eliminate the need for additional turboshaft engines, it was determined that the convertible engine was the best decision. Although this does require the need for an additional transmission shaft, this reduces the vehicle weight by 1,000 lb in comparison to the case in which turboshaft engines were used to drive the rotors. Additionally, due to the need to cross-shaft the rotors with the turboshaft con guration, the margin in weight reduction increases with the convertible engine as the same shafts would already be used in the convertible engine con guration as well.

Since the vehicle should operate out of contested environments, it was determined that One Engine Inoperable (OEI) capability would be valuable for Harpy. Although OEI would require the addition of a second engine, a rudder size/de ection capable of o setting the induced yaw moment, a transmission system capable of driving the rotor shafts via one engine, and a fuel cuto s, the additional survivability and performance the OEI capability o ers is more than commensurate.

Should Harpy lose an engine, clutches at the output shaft of each engine will disconnect the a ected engine, allowing the operable engine to take over power and thrust duties. Additionally, due to the proximity of each engine to centerline, the induced yaw due to the lateral thrust imbalance is minimal and the vehicle has su cient capability during OEI operation.

Two primary engine placements were considered, wing or fuselage mounted. Wing mounted engines would require a standalone nacelle which would greatly impact drag at high speeds, thus the fuselage mount position was determined to be the most approrpiate forHarpy.

Once this was determined, the extent to which the engine would be integrated into the fuselage was considered. The engine could either be o set from the fuselage, or fully/partially integrated with the fuselage. O set from the fuselage would once again generate a considerable amount of nacelle drag, and require an additional engine output shaft perpendicular to the length of the engine. Thus, the engines were partially integrated into the fuselage as well as to permit the fan shafts to extend towards the transmission box illustrated in Fig. 9.3. Note that due to this partial integration an S-duct, shown in Fig. 9.2 was needed to allow air ow into the engines.

9.2 Engine Selection Procedure

Engine selection was carried out by parsing through a database of available jet engines [43] containing an extensive catalog of civilian and military turbofan engines. The primary considerations for engine selection were the cruise thrust requirement and the combined engine-fuel weight.

The cruise thrust requirement was determined with steady-level ight equations and is readily seen in Section 5 while the combined engine-fuel weight was determined by adding the engine weight to the fuel weight the engine would require to complete the mission pro le. Fuel weight was initially approximated using the Breguet range equation in conjunction with the associated engine's TSFC.

The nal engine was selected by removing the engines from a database of jet engines [43] that did not meet the continuous thrust requirement and sorting for the lowest combined engine-fuel weight. This procedure yielded the CF34 engine, shown in Figure 9.1 which has a max continuous thrust of 15,000 lbs.

The CF-34 is consistent with what one would expect for an aircraft ofHarpy's size and application, as seen on the Bombardier CRJ200 in Figure 9.1, which has similar design range, speed, and gross weight as Harpy.

To minimize the weight penalties of separate engines for rotary-wing and xed-wing modes, a convertible turboshaft/turbofan engine type was selected [3, 44]. Given this constraint, it was determined that a set of two CF34 turbofan engines with this technology applied would best suit the vehicle and mission requirements. The engines are partially encased in the fuselage near the tail and fed air ow via an S-duct inlet as seen in Figure 9.2. An S-duct was chosen not only to reduce vehicle observables but also to mount the inlet high, thereby mitigating FOD ingestion more e ectively than a comparable nacelle or wing mounted inlet.

The engines provide the thrust required to overcome the 6,100 lbs (1,371 N) of drag experienced at the 450 KTAS (833.4 km/h) forward ight cruise, discussed more in Section 9.3 Installed Thrust Performance. The engines also provide the shaft power required to drive the rotors during takeo and hover. This is

Figure 9.1 The CF34-3B1 engine and the Bombardier CRJ200

Figure 9.2 Vehicle S-duct Diagram

accomplished via a convertible engine technology demonstrated by NASA in 1996 that extracts additional shaft power from the fan rotor using inlet guide vanes, discussed more in Section 9.4.1 Convertible Engine Description. The power is driven to the rotors via the rotor transmission system seen in Figure 9.3, which replaces the need for additional turboshaft engines to drive the motors.

Figure 9.3 Vehicle Drive Shaft and Transmission System Diagram

9.3 Installed Engine Performance

Installed propulsion system data was evaluated by applying correction factors consisting of bleed air requirements and airframe interference to the uninstalled engine data. The installed and installed system metrics are displayed in Table 9.1.

Bleed air is used to provide power to the Cabin Management System (discussed in Section 9.6))). The correction factor for the bleed air can be found using Equation 1)) [29], where C_B is 2.0 and the mass flow rate ratio ($\dot{m}_B / \dot{m}_E$) is commonly around 0.01 [45]. This gives a thrust correction factor of approximately 0.98.

$$1 \quad \frac{T_{inst}}{T_{uninst}} = C_B \left(\dot{m}_B / \dot{m}_E\right) \tag{1}$$

In Harpy, most of the airframe interference comes from the fuselage-mounted location of the engines on the aircraft. Aircraft with similar S-ducted engines encounter approximately 2% reduction in thrust due to the inlet.

Based on this information, the total installed engine losses are approximately 4%, the calculated installed engine parameters are compared to the uninstalled counterparts in Table 9.1.

Engine Config	Dry Weight	Max Thrust	TSFC
Installed	2,000	15,000	0.346
Uninstalled	2,000	14,350	0.360

Table 9.1 Installed engine performance correction

9.4 Turbofan to Turboshaft Convertible Engine

9.4.1 Convertible Engine Overview

In 1996, NASA tested a concept for a convertible turbofan engine. This conversion allowed shaft power to be extracted from the fan shaft by blocking off the engine bypass ducts with variable guide vanes. By extracting this power to drive a shaft, the engine can be effectively converted between a turbofan and turboshaft engine.

This is useful for Harpy as without it, separate engines for thrust and shaft power would be required. Having separate engines would signi cantly penalize the vehicle as during all mission segments as a signi cant portion of the propulsion system would be functionally unusable while still adding to the total weight of the system.

9.4.2 Power Extraction Mechanics

As previously stated, the turbofan convertible engine is able to operate as a turboshaft engine by extracting shaft power from the fan shaft. This is done by de ecting a set of 30 variable inlet guide vanes (VIGW) installed ahead of the fan rotor, which when de ected are able to unload the fan in the turboshaft mode. These guide vanes have a de ection range of 0 deg (fully open, straight ahead) to +84 deg (nearly closed) to almost suppress the fan ow fully . Note that The core/bypass ow splitter was extended forward to the VIGV to minimize core inlet ow distortion from the de ected VIGV . This engine con guration including the power output shaft and VIGW can be seen below in Figure 9.4 [3].

Figure 9.4 Convertible engine diagram from [3]

9.4.3 Power Extraction Model

To help represent this thrust to power conversion numerically, a model was created to approximate how much shaft power could be extracted from a given amount of thrust. This is needed to calculate both the maximum shaft power (max rate of climb) as well as correlate the power speci c fuel consumption to the given engine speci c fuel consumption. The process the model uses to make this approximation as well its results in comparison to the experimental results can be seen below.

9.4.4 Model Creation

The model begins by using momentum transport to treat the engine thrust as approximately equal to approximately the mass ow rate times the di erence between the inlet and exhaust ow velocities in Equation 2). For the sake of simplicity, the engine is assumed to be static. This allows the engine velocity to be neglected and utilize the static air ow value found in the database for the mass ow rate [43]. Based on this assumption, thrust is a function of only the exit velocity ue. Inversely, the engine exit velocity can be computed from the thrust produced by the engine seen in Equation 2.

$$T = \dot{m}_a (u_e - u_a) \tag{2}$$

To represent the shaft power, the goal is to compute the amount of usable power that can be extracted to bring the overall engine to next zero thrust. This net zero thrust is what would generally be seen in a turboshaft engine.

Equation 3) represents the maximum power extraction from this turbine, where T_{oe} is simple the ambient static temperature at 20,000 ft (6,096 m) as it was assumed that the engine is at rest (allowing it to be read as the static instead of stagnation temperature), C_p is assumed to be constant at the ambient temperature of 20,000 ft (6,096 m), and the mass flow rate is known. This leaves T_{0_6}, the stagnation temperature prior to the turbine, as the only needed quantity to determine the power extraction available to reach net zero thrust. This level of power extraction from the fan shaft is infeasible. Based on common engine design practices, a reasonable power extraction ratio of 0.28 (power extraction per power available) will be applied as a correction factor.

$$P = \dot{W}_{turbine} = (T_{0_6} - T_{0_e})(\dot{m}_a C_{P_{turbine}}) \tag{3}$$

Given the above correlations, a relationship between exit velocity and stagnation temperature is required to fully define the power thrust relationship. This can be seen in Equation 4) which uses TS Diagram methods to construct a formula of the exit velocity in terms of the stagnation temperature and known quantities. Note that Po6, the stagnation pressure prior to the turbine is calculated using the ambient static pressure, ambient air density, and the original exit velocity.

$$u_e = \sqrt{2 C_{p_n} T_{0_e} \left[1 - \left(\frac{P_e}{P_{0_6}} \right)^{\frac{n-1}{n}} \right]} \tag{4}$$

Finally, with all this information, a given thrust to an associated power can be related through the following process. First, Equation 2) relates thrust to exit velocity. Second, Equation 4) relates exit velocity to stagnation temperature before the turbine. Finally, the maximum power extraction is calculated across the turbine using Equation 3) and applyiedthe shaft extraction correction factor to be left with the final power extraction.

The ratio of power extraction per unit thrust varies due to the P_{o_6} value In Equation 4) changing with the square of exit velocity. But given the range of possible exit velocities (zero to max thrust), the ratio of horsepower to pound of thrust ranges between 0.84 and 0.98 using this model.

9.5 Model-Experiment Comparison

This model aligns very well with the general trends that can be seen in the experimental results. For example, when comparing the engine experimental test path (shown in Figure 9.5a) to the curve generated by the model (shown in Figure 9.5b), they both follow a similar trend.

Additionally, when comparing the linear regions (higher thrust and lower power output) of both the model and the experimental results, the power to thrust tradeoff values are close as well. As previously discussed in Section 9.4.4 the ratio of horsepower to pound of thrust (hp/lb) utilizing the model ranges between 0.84 and 0.98. In comparison, utilizing the information shown in Figure 9.5a as well as other data shown in the experimental results, the experiment showed a ratio of horsepower to pound of thrust approximately between 0.75 and 1 [3].

Given this information, and the support of experimental results, this model seems to be a reasonable method for approximating the power to thrust conversion of the convertible engine.

(a) Experimental results from [3] (b) Model results

Figure 9.5 Power vs Thrust Trade-o for Convertible Engine

9.6 Cabin Management System

The vehicle is required to be pressurized to 8,000 ft (2,438 m) while at 20,000 ft (6,096 m) cruise, so a cabin management system was introduced. The cabin management system is decomposed into two primary sections: the Cabin Pressurization System (CPS) and the Cabin Conditioning System (CCS).

The Cabin Pressurization System (CPS) functions to pressurize the main cabin to 8,000 ft (2,438 m) during the ascent phase of the mission and while at 20,000 ft (6,096 m) cruise. It does this by extracting bleed air from the turbofan engines and ambient air through two ram air holes and feeding this air into the ow control valve which modulates each of these ows. From the ow control valve, the air is fed into the Cold Air Unit (CAU) and enters the main cabin. This system is referred to as a Pressurization Air Conditioning Kit (PACK). There is one PACK for each engine and the equipment is housed in the wing to body fairing. Depending on the cabin conditions, there is an out ow valve that modulates the release of air from the cabin to maintain a pressurization of 8,000 ft (2,438 m). See Fig. 9.6) for a owchart describing the CPS. See Figure 9.7) for a diagram of how the system is laid out within the vehicle.

Figure 9.6 Cabin Pressurization System Flowchart

The Cabin Conditioning System (CCS) functions to maintain cabin temperature and prevent the aircraft fuel from freezing as the external air temperature is approximately -12F (-24.4 C) at 20,000 ft (6096 m) ISA. The heat for these tasks is sourced from the previously discussed PACKs. The heat from the Heat Exchanger (Fig. 9.6) is primarily extracted by exposing the engine bleed air to the fuel tanks. To modulate

Figure 9.7 Cabin Pressurization Vehicle Layout

the remaining heat and the resulting cabin temperature, the ow control valve varies the mixture of bleed air and ram air that is introduced into the PACKs to achieve the required temperature.

10 Computer Aided Design

Along with the three-view representations of the vehicle hover mode and forward ight mode shown earlier in the report, more speci c and important parameters are delineated in Table 10.1.

Parameter	English	SI
Forward Flight Span	100 ft	30.48 m
Rotor Radius	18 ft	5.49 m
Rotor Root Chord	6 ft	1.83 m
Wing Sweep	20	20
Wing Dihedral	3	3
Wing Root Chord	15.86 ft	4.83 m
Wing Tip Chord	11.25 ft	3.429 m
Fuselage Length	89.1 ft	27.16 m
Fuselage Maximum Width	15 ft	4.57 m
Fuselage Maximum Height	12 ft	3.66 m

Table 10.1 Important vehicle parameters.

10.1 Fuselage Internal Pro le

The payload t (pink region) was the driving factor for the internal fuselage geometry. To illustrate this, Figure 10.1 displays a few angles and cross sections of the internal structure surrounding the required payload.

Figure 10.1 Multiple view of the payload inside the vehicle.

Additionally, the fuel tank, landing gear, and internal oor were also modeled and can also be seen in Fig. 10.1. The current fuel tank design has a volume of 320 ft^3 (9.06 m^3) and was placed under the fuselage (yellow region) to lower the center of gravity since the wing is mounted above the fuselage. A traditional bicycle landing gear was chosen to reduce internal space required while still o ering su cient structural rigidity.

10.2 Wing Sliding Door for Stowing Rotor

To minimize drag, the retreating blades are stored during forward ight, employing a sliding door along the wing upper surface. The wing itself has an open bay area that permits the rotor to be elastically restrained. This bay area is accessed with a sliding door that moves inboard under the skin of the wing when opening and is ush with the wing skin when closed, as illustrated in Fig. 10.2.

Figure 10.2 Procedural picture of the rotor door sliding inboard for opening the rotor bay area. The QR codes links to a animations of the rotor tilt mechanisms (left) and sliding door motion (right).

10.3 Cargo Ramp

For loading and unloading payload, a traditional cargo ramp was selected. Special care was taken to insure that the payload can be loaded into the cargo bay at the angle the ramp rests at. An image of the component can be seen in Figure 10.3.

Figure 10.3 Rear cargo ramp.

10.4 Forward and Aft Rotor Tilt

For added control of the vehicle, along with the lateral outboard tilt of the rotor, the nacelles are able to tilt the rotor forward and aft. This motion is limited to 5 forward and 5 aft. This motion on the vehicle is shown in a video available by scanning the left QR code in Fig. 10.2.

10.5 Vehicle Landing Con gurations

The Harpy is able to land both in VTOL and conventional xed-wing modes, as illustrated in Fig. 10.4. Operationally, the VTOL mode is the mission requirement, but the conventional landing provides an